Molecular Crystals and Liquid Crystals

ISSN: 1542-1406 (Print) 1563-5287 (Online) Journal homepage: http://www.tandfonline.com/loi/gmcl20

Influence of Pentacene Film Thickness on Environmental Stability of Pentacene Thin-Film Transistors

Jin-Hyuk Kwon, Xue Zhang, Ji-Ho Park, Do-Kyung Kim, Jaehoon Park & Jin-Hyuk Bae

To cite this article: Jin-Hyuk Kwon, Xue Zhang, Ji-Ho Park, Do-Kyung Kim, Jaehoon Park & Jin-Hyuk Bae (2015) Influence of Pentacene Film Thickness on Environmental Stability of Pentacene Thin-Film Transistors, Molecular Crystals and Liquid Crystals, 620:1, 10-20, DOI: 10.1080/15421406.2015.1094611

To link to this article: http://dx.doi.org/10.1080/15421406.2015.1094611

Published online: 16 Dec 2015.

Mol. Cryst. Liq. Cryst., Vol. 620: pp. 10–20, 2015

ISSN: 1542-1406 print/1563-5287 online
DOI: 10.1080/15421406.2015.1094611

Influence of Pentacene Film Thickness on Environmental Stability of Pentacene Thin-Film Transistors

JIN-HYUK KWON,[1] XUE ZHANG,[2] JI-HO PARK,[2] DO-KYUNG KIM,[1] JAEHOON PARK,[2,*] AND JIN-HYUK BAE[1,*]

[1]School of Electronics Engineering, Kyungpook National University, Daegu, Republic of Korea
[2]Department of Electronic Engineering, Hallym University, Chuncheon, Republic of Korea

We investigated the influence of pentacene film thickness on the environmental stability of thin-film transistors (TFTs). In order to evaluate the environmental stability, the transfer and output characteristics in pentacene TFTs were measured in air and vacuum environments. The pentacene-thickness-dependent variation of transfer characteristics was shown to originate from the fixed charge at the pentacene/polymeric insulator interface induced by air molecules. In addition, an analysis of parasitic resistance suggests that air molecules degraded the contact property and increased channel conductivity. Particularly, a thick pentacene film was found to passivate the TFT channel region interrupting the penetration of air molecules.

Keywords Pentacene; Thin-film transistor; Environmental stability; Pentacene film thickness.

Introduction

In the past decade, a significant number of studies were conducted on organic thin-film transistors (TFTs) because of their potential application to various flexible and cost-effective electronic devices such as active matrix displays, sensors, smart cards, and radio frequency tags [1−4]. In particular, from the viewpoint of compatibility with flexible substrate, organic TFTs with polymeric insulators fabricated by a solution process have been studied more extensively, compared to those with inorganic gate insulators. As a consequence of the numerous studies in various research fields, the magnitude of field-effect mobility in organic TFTs, which is one of the decisive factors for the substitution of conventional non-flexible inorganic transistors, eventually became comparable to or exceeded the value in conventional silicon-based transistors [5−8]. Although organic TFTs with high electrical properties are already competitive as low-cost, flexible products, some issues remain to be

*Address correspondence to Jaehoon Park, Department of Electronic Engineering, Hallym University, 1 Hallymdaehak-gil, Chuncheon, Gangwon-do 200-702, Korea, E-mail: jaypark@hallym.ac.kr, and Jin-Hyuk Bae, School of Electronics Engineering, Kyungpook National University, Daegu 702-701, Korea, E-mail: jhbae@ee.knu.ac.kr.

Color versions of one or more of the figures in the article can be found online at www.tandfonline.com/gmcl.

solved for enabling their practical application in the industrial market. For example, the environmental instability of organic TFTs in ambient air, which has detrimental effects on the TFT current on/off ratio, mobility, and subthreshold voltage in terms of device stability and uniformity [9−11], remains problematic. In order to overcome such a limitation, we need a comprehensive and multidimensional understanding of the effects of the environment on the electrical properties of organic TFTs.

In this work, we describe the influence of pentacene film thickness on the environmental stability of pentacene TFTs. For generating different environmental conditions, the electrical characteristics of the pentacene TFTs were obtained in both ambient air and vacuum. By measuring the transfer characteristics, the field-effect mobility, threshold voltage shift, and on-off state drain current were systematically examined to analyze the interactions between air molecules and the pentacene/polymeric gate insulator interface from the viewpoint of interfacial charge. Furthermore, in order to examine the contact property in air and vacuum, the total resistance of the TFT was also calculated from the linear region of output characteristic curves.

Experimental

Pentacene TFTs with polymeric gate insulators were fabricated with a top contact and bottom gate structure in this study. A 40-nm-thick Al gate electrode was thermally evaporated onto a glass substrate through a shadow mask. The poly(methyl methacrylate) (PMMA) solution (approximately 4.8 wt.% dissolved in anisole) was spin-coated on to the Al-patterned substrate to form a gate insulator, and cured for 60 min at 120°C; the resulting thickness was approximately 150 nm. Pentacene, the active layer, was then thermally evaporated onto the PMMA layer to thicknesses of 20, 30, and 40 nm through different shadow masks. The substrate was kept at room temperature, and the deposition rate was approximately 0.05 nm/s.

The fabrication of the top-contact pentacene TFT was completed by depositing 40-nm-thick Au source (S) and drain (D) electrodes through another shadow mask. The channel length (L) and width (W) were 200 μm and 4000 μm, respectively. Subsequently, electrical measurements of the fabricated transistors were performed by changing the ambient condition from air to vacuum and back to air using an HP 4140B picoammeter/voltage source.

Results and Discussion

Figure 1 shows the transfer characteristic curves of the pentacene TFTs with pentacene thicknesses of 20, 30, and 40 nm. The transfer curves were obtained at a fixed drain voltage (V_D) of −20 V, and the gate voltage (V_G) was swept from 15 V to −40 V and back to 15 V in −0.5 V increments. The measurement was performed thrice for each device; by changing the ambient condition of the devices from air to vacuum and back to air. Note that successive measurements under different ambient conditions were carried out without any time interval in order to minimize time-dependent variation. As shown in Figure 2, for all devices, the off-state drain current (I_D) in vacuum dropped below the initial measured current in air, and increased immediately after re-exposure to air. This indicates that air molecules penetrate into the pentacene film and induce an increase in current, which might also cause the slightly higher on-state drain current at high gate voltages. With regard to the influence of pentacene thickness, the off-state drain current of the TFTs with 30 nm-thick

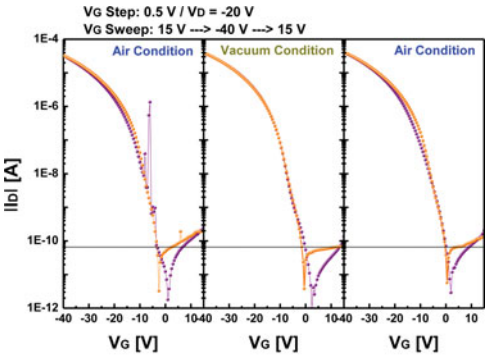

(a)

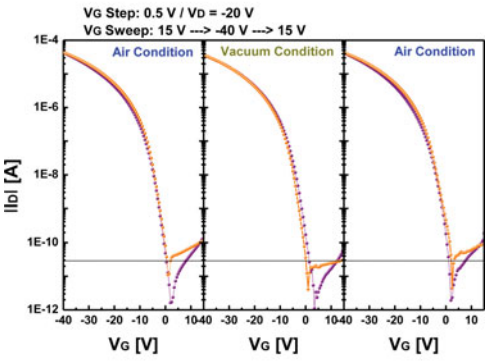

(b)

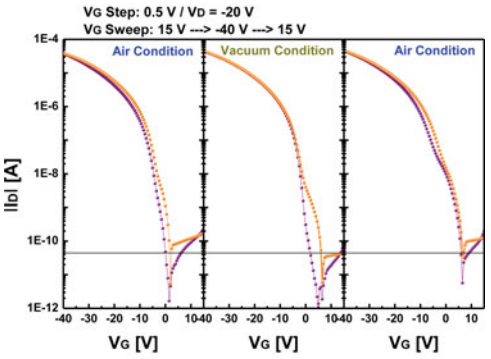

(c)

Figure 1. Transfer characteristics (log $|I_D|$ versus V_G plots, at $V_D = -20V$) of our pentacene TFTs with active layer thicknesses of (a) 20 nm, (b) 30 nm and (c) 40 nm under different measuring environments; 1st data in ambient air, 2nd data in vacuum, and 3rd data in ambient air.

pentacene layers immediately recovered to its initial air value, whereas that of the other devices did not return to the initial value measured in air.

Figure 3 shows the variation in mobility due to the reversal of the gate voltage sweep direction, for which the field-effect mobility was calculated in the saturation region and that

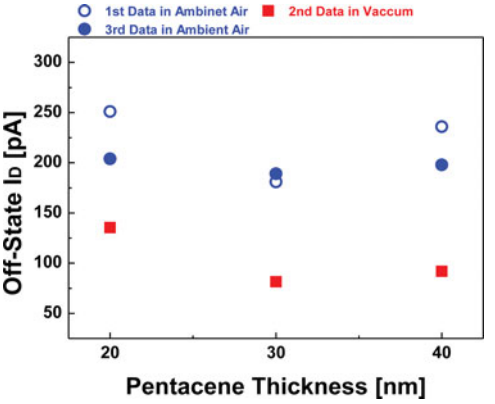

Figure 2. Off-state drain current of our pentacene TFTs as a function of pentacene film thickness; 1st data in ambient air, 2nd data in vacuum, and 3rd data in ambient air.

obtained by sweeping the gate voltage from −40 V to 15 V was then divided by one obtained by sweeping the gate voltage from 15 V to −40 V. Herein, after the first measurement, those for the 20-, 30-, and 40-nm-thick pentacene devices were 0.30, 0.29, and 0.26 cm^2/Vs, respectively. In contrast to the vacuum case, the field-effect mobility was severely varied by the gate voltage sweep in air. Unlike the TFTs with 20 nm- and 40 nm-thick pentacene layers, the mobility variation in the TFT with the 30 nm-thick pentacene layer was promptly restored to its initial value after re-exposure to ambient air. In addition, the initial mobility variation in air of the TFT with the 40 nm-thick pentacene layer was more severe than that of the other TFTs. However, the mobility variation in the case of the 30 nm-thick pentacene layer became most severe, after re-exposure to ambient air. Throughout the measurements, the mobility variation was least severe in the case of the 20 nm-thick pentacene layer.

The threshold voltage (V_T) shift was also analyzed upon the reversal of the gate voltage sweep direction. Figure 5 presents the threshold voltage shift, which was obtained from a plot of the square root of $|I_D|$ versus V_G shown in Figure 4. In the air condition before and

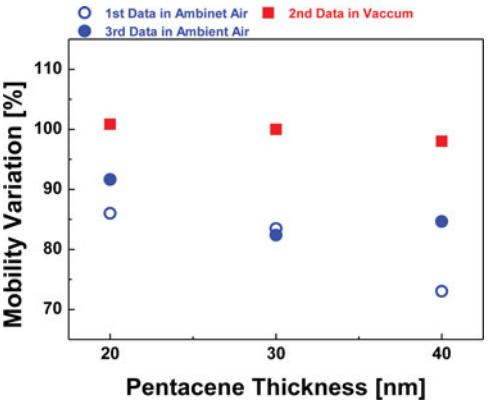

Figure 3. Mobility variation of our pentacene TFTs upon the reversal of the gate voltage sweep direction as a function of pentacene film thickness; 1st data in ambient air, 2nd data in vacuum, and 3rd data in ambient air.

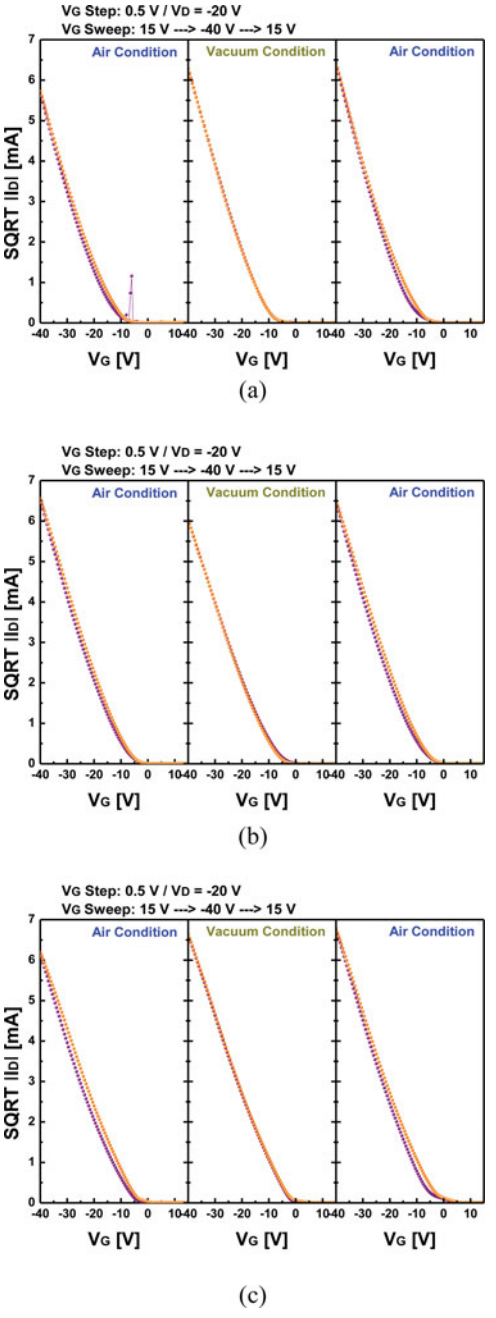

Figure 4. Threshold voltage shift and fixed charge density of our pentacene TFTs as a function of pentacene film thickness; 1st data in ambient air, 2nd data in vacuum, and 3rd data in ambient air.

after vacuum treatment, all devices exhibited a positive shift in threshold voltage, whereas no considerable change in the threshold voltage was observed under the vacuum condition. On the basis of the threshold voltage shift, the density of fixed charge generated at the

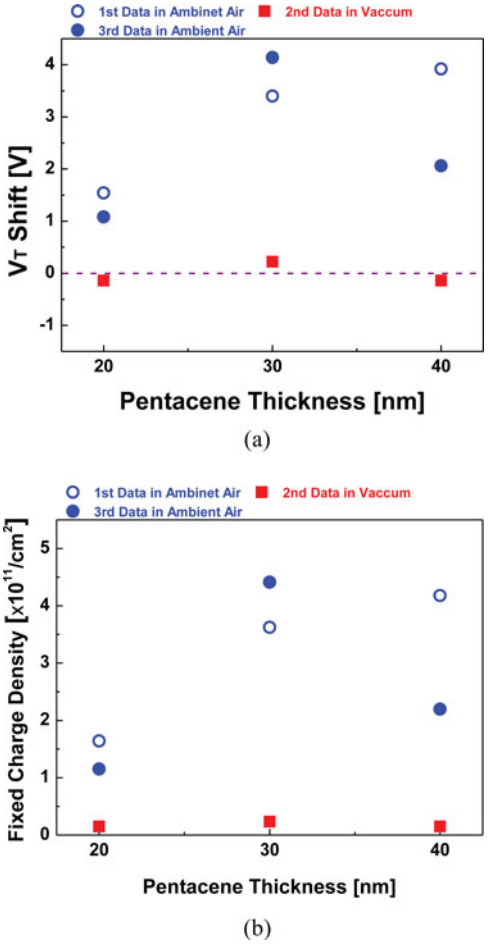

Figure 5. Transfer characteristics (sqrt $|I_D|$ versus V_G plots, at $V_D = -20V$) of our pentacene TFTs with active layer thicknesses of (a) 20 nm, (b) 30 nm, and (c) 40 nm under different measuring environments; 1st data in ambient air, 2nd data in vacuum, and 3rd data in ambient air.

pentacene/PMMA interface was calculated by using the following equation

$$Q_{it} = \Delta V_T \times C_i$$

where C_i is the dielectric capacitance of PMMA (approximately 17 nF/cm^2, measured in air). The case of the 20 nm-thick-pentacene layer consistently showed the lowest density of interfacial fixed charge. In the air condition, although the case of the 40 nm-thick pentacene layer showed the highest density of interfacial fixed charge before vacuum treatment, the fixed charge density of the case of the 30 nm-thick pentacene layer was higher than that of the 40 nm case after breaking the vacuum. The generation of interfacial fixed charge may be associated with polar molecules such as H_2O, which penetrate the pentacene film and result in a non-uniform polarization condition at the pentacene/PMMA interface [12]. Note that polar molecules are known to act as charge-trap sites in organic TFTs. The relatively slow recovery of the 40 nm case can be attributed to the self-passivation

of the relatively thick pentacene film. The 20 nm case might be an exception because of the relatively small amount of air molecules it contains. The fixed charge density of the TFT with the 30 nm-thick pentacene layer increased after the vacuum treatment and exceeded its initial value measured in air, whereas the fixed charge densities in the cases of the 20 nm- and 40nm-thick pentacene layers did not increase up to their initial values. Interestingly, such a unique behavior in the case of the 30 nm-thick-pentacene layer was also observed in the results of the off-state drain current and the mobility variation. Considering that the off-state drain current and mobility variation were obtained from the transfer characteristics of the TFTs, the transition behaviors of the off-state current and mobility may originate from the variation of interfacial fixed charge resulting from the successive measurement under different ambient conditions. As shown in Figure 6, noticeable clockwise hysteresis was observed under the air condition for all devices. The clockwise hysteresis might be caused by the release of holes captured by polar H_2O molecules, which contributes to the current, as the gate voltage is swept in the reverse direction [12]. This hysteresis behavior nearly disappeared when the devices were kept in vacuum.

The output curves shown in Figure 7 were obtained at a fixed gate voltage of -10 V, while the drain voltage was swept from 0 V to -50 V and back to 0 V in -0.5 V increments. For all the devices, the magnitude of the drain current dramatically increased in vacuum. The drain current did not recover to its initial value in the second measurement in air. Rather, the re-exposure to air immediately caused the drain current to increase further. The current increase is related to the relatively low density of defect states in the source and drain contacts together with the enhanced dielectric capacitance caused by air molecules [13]. Additionally, a reduction in drain saturation current occurred upon the reversal of the gate voltage sweep direction after re-exposure to air. This is indicative of the presence of polar air molecules in pentacene film, which could interrupt the flow of holes upon the reversal of the drain voltage sweep direction.

In order to examine the charge injection property, parasitic resistance values ($R_{Parasitic}$) of the fabricated pentacene TFTs were extracted from the linear region of their output curves by using the relationship of $\partial V_D/\partial I_D$ [14]. Figure 8 presents the extracted parasitic resistance which was multiplied with the channel width (W). For all devices, the parasitic resistance was shown to be reduced after the TFT was kept in vacuum. This is indicative of an enhancement in the contact property between Au source/drain electrodes and the pentacene film, because the polarization of the gate insulator is fixed during the output measurement, as the gate voltage is constant. Therefore, the dramatic increase in the drain current in vacuum can be attributed to the reduction of the parasitic resistance in the pentacene TFT. Note that the parasitic resistance is the sum of the contact resistance, bulk resistance, and channel resistance of the TFT. Because the gate insulator/pentacene interface is not significantly different in different devices, such a reduction in the parasitic resistance is assumed to be related to the contact resistance reduction. This explanation is supported by the measurement of transfer characteristics. In contrast to the output characteristics, the transfer characteristics did not show a considerable current variation resulting from the different ambient conditions.

The contact resistance variation was found to have a remarkable dependency on the thickness of the pentacene film. As can be seen in Figure 8, the TFT with the 20 nm-thick pentacene layer, showed the widest variation in parasitic resistance after it was kept in vacuum. After re-exposure to air, the parasitic resistance decreased below the value measured in vacuum for the 20 nm and 30nm cases. The reduction of parasitic resistance in the 20 nm and 30 nm cases after re-exposure to air is assumed to be due to the air molecules

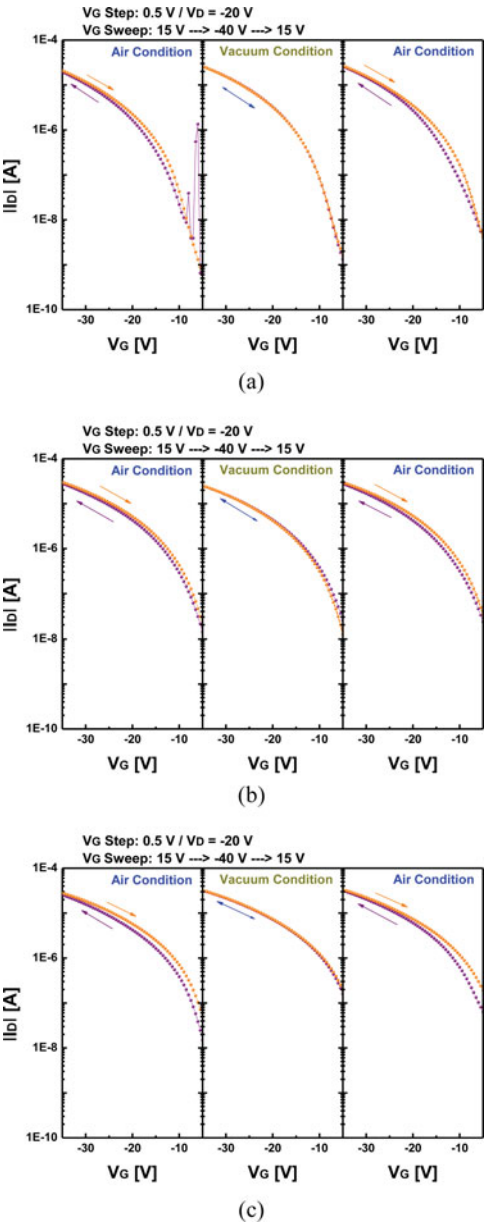

Figure 6. Hysteresis behaviors (log $|I_D|$ versus V_G plots, with V_G ranging from -5 V to -35 V) of our pentacene TFTs with active layer thicknesses of (a) 20 nm, (b) 30 nm, and (c) 40 nm under different measuring environments; 1st data in ambient air, 2nd data in vacuum, and 3rd data in ambient air.

that penetrated the channel region, resulting in the enhancement of channel conductivity. Note that the difference between the second data in vacuum and the third data in air tends to attenuate for thicker pentacene films, and the diffusion of air molecules under the source and drain contacts is known to be a relatively slow process [12].

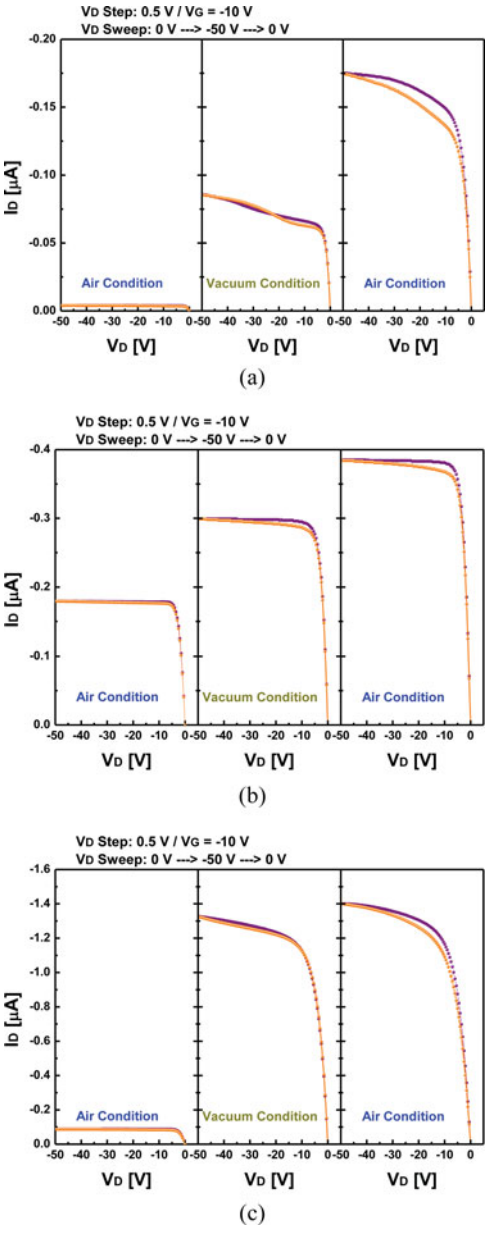

Figure 7. Output characteristics (I_D versus V_D plots, at $V_G = -10$ V) of our pentacene TFTs with active layer thicknesses of (a) 20 nm, (b) 30 nm, and (c) 40 nm under different measuring environments; 1st data in ambient air, 2nd data in vacuum, and 3rd data in ambient air.

Conclusion

We fabricated top-contact pentacene TFTs with a PMMA gate insulator. The pentacene films were deposited through thermal evaporation. Measurements were performed by changing

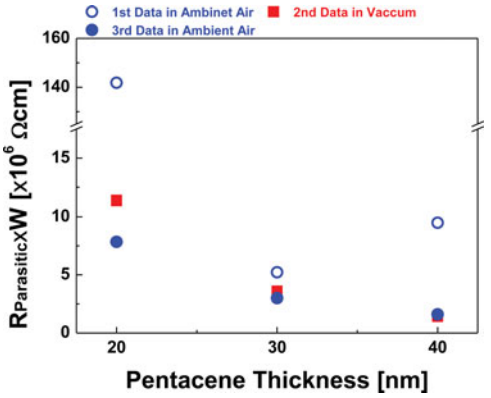

Figure 8. Parasitic resistance of our pentacene TFTs as a function of pentacene film thickness; 1st data in ambient air, 2nd data in vacuum, and 3rd data in ambient air.

the ambient condition from air to vacuum and back to air. An analysis of transfer characteristics from the viewpoint of fixed charge at the pentacene/PMMA insulator interface suggests that the key performance parameters, field-effect mobility and threshold voltage are varied by polar air molecules that penetrate the pentacene film, and the environmental stability of the parameters have a dependency on pentacene film thickness. In particular, after re-exposure to air, the parasitic resistance decreased below the value measured in vacuum for the cases of the 20 nm and 30 nm-thick pentacene layers, in contrast to the 40 nm case. This suggests that a thick pentacene film passivates the TFT channel region interrupting the penetration of air molecules.

Acknowledgements

This work was supported by Hallym University Research Fund (HRF-G-2015-1) and Basic Science Research Programs through the National Research Foundation of Korea (NRF) funded by the Ministry of Education (2013R1A1A4A01009807 and 2014R1A1A2057057). This research was also supported by Global Ph.D. Fellowship Program through the NRF funded by the Ministry of Education (2014H1A2A1021666).

References

[1] Someya, T., Kato, Y., Sekitani, T., Iba, S., Noguchi, Y., Murase, Y., Kawaguchi, H., & Sakurai, T., (2007). *Natil. Acad. Sci. USA 102*, 104515 .

[2] Rotzoll, R., Mohapatra, S., Olariu, V., Wenz, R., Grigas, M., Dimmler, K., Shckekin, O., & Dodabalapur, A., (2006). *Appl. Phys. Lett. 88*, 123502 .

[3] Zhou, L., Wanga, A., Wu, S.-C., Sun, J., Park, S., & Jackson, T. N. (2006). *Appl. Phys. Lett. 88*, 083502 .

[4] Tsukagoshi, K., Tanabe, J., Yagi, I., Shigeto, K., & Yanagisawa, K. (2006). *J. Appl. Phys. 99*, 064506 .

[5] 25th Anniversary Article: organic Field-Effect Transistors: The path Beyond Amorphous Silicon, Henning Sirringhaus, *Adv. Mater. 26*, 1319 (2014).

[6] Kinoshita, S., Sakanoue, T., Yahiro, M., Takimiya, K., Ebata, H., Ikeda, M., Kuwabara, H., & Adachi, C. (2008). *Solid State Comm. 145*, 114

[7] Haas, S., Takahashi, Y., Takimiya, K., & Hasegawa, T. (2009). *Appl. Phys. Lett. 95*, 022111

[8] Klauk, H., Zschieschang, U., Pflaum, J., & Halik, M., (2007) *Nature 445*, 745
[9] Weitz, R.T., Amsharov, K., Zschieschang, U., Burghard, M., Jansen, M., Kelsch, M., Rhamati, B., van Aken, P.A., Kern, K., & Klauk, H. (2009). *Chem. Mater*. *21*, 4949 .
[10] Simeone, D., Rapisarda, M., Fortunato, G., Valletta, A., & Mariucci, L. (2011). *Org. Electron. 12*, 447 .
[11] Bae, J.-H., Park, J., Keum, C.-M., Kim, W.-H., Kim, M.-H., Kim, S.-O., Kwon, S.K., & Lee, S.-D. (2010). *Org. Electron. 11*, 784 .
[12] Kumaki, D., Umeda, T., & Tokito, S. (2008). *Appl. Phys. Lett. 92*, 093309 .
[13] Park, J., Do, L.-M, Bae, J.-H, Jeong, Y.-S, Pearson, C., & Petty, M. C. (2013). *Org. Electron. 14*, 2101.
[14] Meijer, E. J., Gelinck, G. H., van, E. Veenendaal, Huisman, B.-H., Leeuw, D. M. de, & Klapwijk T. M. (2003). *Appl. Phys. Lett. 82*, 4576 .